Preferred orientation of chopped fibers in polymer-based composites processed by selective laser sintering and fused deposition modeling: Effects on mechanical properties

Publisher : John Wiley & Sons, Inc.
Location : Hoboken, USA
DOI : 10.1002/(ISSN)1097-4628
ISSN (print) : 0021-8995
ISSN (electronic) : 1097-4628
ID (product) : APP
Title (main) : Journal of Applied Polymer Science
Title (short) : J Appl Polym Sci

Numbering (journalVolume) : 9999
Numbering (journalIssue) : 9999
DOI : 10.1002/app.49152
ID (unit) : APP49152
ID (society) : app.20193098
ID (eLocator) : e49152
Count (pageTotal) : 12
Title (articleCategory) : ARTICLE
Title (tocHeading1) : ARTICLES

Event (manuscriptReceived) : 2019-11-06
Event (manuscriptRevised) : 2020-02-13
Event (manuscriptAccepted) : 2020-02-13
Event (xmlCreated) : 2020-02-25 (SPi Global)
Numbering (pageFirst) : n/a
Numbering (pageLast) : n/a
Link (toTypesetVersion) : file:app49152.pdf
Link (toAuthorManuscriptVersion) : file:app49152_am.pdf

Short Authors: Badini et al.

Preferred orientation of chopped fibers in polymer-based composites processed by selective laser sintering and fused deposition modeling: Effects on mechanical properties<<Query: As per journal style, abbreviations should be avoided in the article title. Please check and correct if appropriate. Ans: Ok>>

<<Query: Please confirm that given names (blue) and surnames/family names (vermilion) have been identified and spelled correctly. Ans: I would like to add the secon name of one author: Vito Lambertini should become Vito Guido Lambertini. Affiliation:Group Materials Labs-Polymers, Centro Ricerche Fiat

S.C.p.A, Torino, Italy>>Claudio<<Query: Please check if link to ORCID is correct. Ans: The link to ORCID is correct >> Badini[1], Elisa Padovano*[1], Rosario De Camillis[1], Vito Lambertini[2], Mario Pietroluongo[1]

[1] Department of Applied Science and Technology, Politecnico di Torino, Torino, Italy

[2] Group Materials Lab-Polymers, Centro Ricerche FIAT, Torino, Italy

Elisa Padovano: ✉ elisa.padovano@polito.it

*Correspondence to:

<<Query: Please check the affiliations and correspondence details for accuracy. Ans: Affiliations and correspondence details are correct >>Correspondence

Elisa Padovano, Department of Applied Science and Technology, Politecnico di Torino, Corso Duca degli Abruzzi 24, 10129 Torino, Italy.

Email: elisa.padovano@polito.it

Abstract

The orientation of reinforcing fibers in polymer-based composites greatly affects their mechanical features. It is known that different orientations of continuous fibers in the stacked layers of a laminate play a crucial role in providing an isotropic mechanical behavior, while the alignment of chopped fibers in injection molding of composites results in a degree of anisotropy. Recent additive manufacturing techniques have offered a way of controlling the fiber orientation. This article aims to investigate the effect of fiber orientation on the mechanical properties of polyamide/carbon fiber composites processed by fused deposition modeling and selective laser sintering. Tensile samples which had different fibers and layer interface with respect to the sample axis (and therefore to the tensile load) were produced. Tensile tests were performed at different strain rates; the tensile properties and the fracture surface morphology were correlated with the processing method and the sample microstructure. The best strength and stiffness were observed when the fibers and the layer interfaces were parallel to the sample axis.

Graphical Abstract

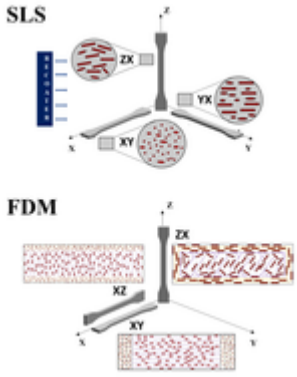

Keywords: composites; mechanical properties; thermoplastics

1 INTRODUCTION

Processing polymers by additive manufacturing (AM) was traditionally exploited for rapid prototyping;[1] however, in more recent years AM has also been considered as suitable for the manufacturing of industrial

products.[2–4] For this reason, many efforts have been made to enhance the performance of AM components through the use of polymers with better mechanical behavior, the addition of strengthening fillers and the improvement of the processing path.[5, 6] These advancements and the flexibility of AM in the design and manufacturing of products have greatly enlarged the application fields of AM components and the number of products available in the market as well.[7–9]

It is well known that the components processed by selective laser sintering (SLS) or by fused deposition modeling (FDM) show properties, which depend on their building parameters. In SLS, the main parameters to be optimized are the laser power, the laser scanning speed and the distance between the scan lines.[10] On the other hand, in FDM technology, the extrusion temperature and the speed of filament deposition play a key role, in addition to the infill percentage and strategy, and the raster angle.[11] In both these technologies, the parts produced can show different mechanical behaviors depending on their orientation on the building platform, because this affects the placement of the layer interfaces.[12, 13] This is closely linked to the nature of additive technologies, which involves the production of a component using a layer-by-layer strategy. The importance of building orientation is further enhanced when processing a fiber-reinforced polymer matrix. In fact, the building orientation likely involves the orientation of the fibers too, which can greatly influence the behavior of the composite material. This effect has been well investigated for composites containing continuous fibers, whose orientation is completely controlled during the FDM process by using two printing heads,[14–17] but also in the case of FDM composite parts containing short fibers the building orientation was found to affect the flexural properties.[18]

Actually, fillers with a high aspect ratio, such as chopped fibers, are expected to show a strong degree of orientation degree in composite parts processed by FDM due to the extrusion process and the deposition of filaments. However, in SLS technology, it was theorized that the fibers orientation depends on the direction of movement of the recoater.[19] The fiber orientation can in fact enhance the anisotropy of the material in terms of mechanical properties and some other physical properties, like thermal conductivity.[20–22] To summarize, anisotropy results from the combination of several effects: part orientation, fiber alignment, and additive manufacturing technique used to produce the components. Since only few studies focus on the anisotropy of composite parts containing chopped fibers and produced by FDM or SLS[18, 19] the importance of fiber alignment in these materials clearly requires further investigation, also by comparing the results given by different additive manufacturing techniques. In this article, the anisotropic mechanical characteristics of polymer/carbon fiber composites processed by SLS and FDM have been investigated and discussed on the base of their microstructure. In particular, three composite materials with a polyamide matrix reinforced with carbon fibers were submitted to 3D printing. For both additive techniques, three different orientations of the specimens with respect to the building platform were taken into consideration.

The present work highlights the way in which the orientation of the printed parts with respect to the building platform effects the mechanical properties. This was correlated to the different alignment directions of the fibers inside the specimens. Understanding this relationship could drive the choice of the more convenient placement of a component under construction inside a building chamber.

2 EXPERIMENTAL DETAILS

Three composite materials constituted by polyamide matrices filled with chopped carbon fibers were processed by additive manufacturing; the resulting microstructure and mechanical behavior were investigated. Tensile specimens of Windform®XT 2.0 and Windform®SP, produced by SLS, were purchased from CRP Technology (Modena, Italy). Windform®XT 2.0 and Windform®SP are composites with matrices of polyamide-12 and polyamide-11, respectively, reinforced with carbon fibers. Carbon PA filaments (polyamide-6/carbon fibers composite, supplied by Roboze, Bari, Italy) were used to manufacture tensile specimens by FDM according to the following processing parameters: extrusion temperature of 300°C, building platform temperature of 45°C, printing speed of 3,000 mm/min, layer thickness of 0.2 mm, raster angle of ±45° and air gap 0. Several sets of specimens were processed according to different building orientations as depicted in Figure 1.

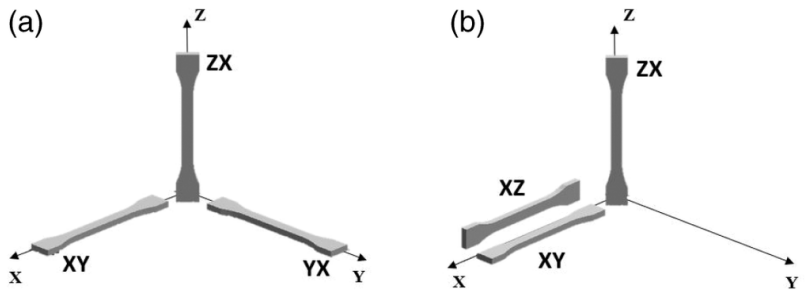

Figure 1 (a) Building orientations adopted for samples processed by SLS: XY, YX, ZX; (b) Building orientations adopted for samples processed by FDM: XY, XZ, and ZX

Each set of samples was labeled by a couple of directions: the first one identifies the direction, which is parallel to the axis of the tensile specimen, while the combination of the two directions identifies the plane in the building chamber where the flat sample lies. For all the specimens, the deposited layers (of powders or filaments) were progressively stacked in *Z* direction, which is the growing direction of the object produced by additive manufacturing. During the SLS process, the recoater always moved in the *X* direction for flattening the powder layer. Then the laser source, which was focused and deflected according to a specific scanning strategy, interacted with the powders and sintered them according to the CAD model. First, the laser sintered the contour of the object under construction and then the layer was completely consolidated by scanning the space inside the contour. During the FDM process, a similar scanning strategy was adopted, but the contour and the infill showed different structure. In FDM technology in fact, each layer is formed through the deposition of a filament and not by a laser scanning; therefore, the direction of the filament deposition (and therefore of the reinforcement, if present) changes during the formation of the contour and of the infill.

Tensile tests were performed on each set of six specimens at the temperature of 23°C by using MTS ALLIANCE FR/100 equipped with a video-extensimeter (10 kN loading cell) and MTS Landmark (25 kN loading cell) dynamometers for static and dynamic tests, respectively. Two strain rates were adopted for the tensile tests, since these testing conditions are currently used for the qualification of semistructural materials in automotive industry. Using the strain rate of 0.1 mm/s makes it possible to assess the material behavior under a static load, while the strain rate of 10 mm/s is used to simulate the effect of an impact under medium or low load (for example the impact of a component when a vehicle is driven in reverse). The static tensile tests were carried out according to ISO 527/1A standard, using flat dog-bone specimens (length 170 mm, gauge length 75 mm, radius 24 mm, and thickness 4 mm). The tests at higher strain rate were carried out by using smaller flat dog-bone specimens (length 60 mm, gauge length 10 mm, radius 12.5 mm, and thickness 3 mm).

The microstructure of the materials (filaments and printed parts) was investigated by using thermal analysis, X-ray diffraction and microscopy. Differential scanning calorimetry (Perkin Elmer, Pyris 1 equipment) was carried out under an argon atmosphere with a flow of 30 ml/min, and using heating and cooling rates of 10°C/min. X-ray diffraction analyses (Panalytical X'PERT PRO PW3040/60, Cu K_α radiation) were used to investigate the crystalline part of the polyamide matrices. Thermal gravimetric tests (TGA/SDTA851 Mettler Toledo) were carried out up to 1,000°C under both argon atmosphere and air (heating rate of 10°C/min, gas flowing at 50 ml/min) in order to study the material degradation and measure the amount of fillers. Samples of printed parts and filaments were then heated under argon in a furnace (Elite Thermal System Limited BSF 11/22, Tersid srl, Italy) to cause the thermal decomposition of the matrix and to collect the remaining carbon fibers. Afterwards, the fibers were observed by an optical microscope (Leica DMI 5000M); about 200 fibers were measured in order to obtain a statistical distribution of their length. The fibers were divided into groups with different average length (each class consisted of fibers with length ranging between mean length-*x* μm and mean length + *x* μm); the numerousness of the fibers in each group was expressed as percent with respect to the total number of fibers. The microstructure of both filaments and specimens processed by additive manufacturing was also investigated. To this purpose, their cross sections (perpendicular to the axis of tensile specimens or filaments) were examined by using optical and scanning electron microscopy (Merlin FESEM, Zeiss). Electron microscopy was also used for investigating the fracture surfaces after the tensile tests.

3 RESULTS AND DISCUSSION

3.1 Characterization of composite materials: Matrices and fibers

The XRD<<Query: Please check hierarchy of section level headings. Ans: Section 3.1 correspond to "Characterization of composite materials: matrices and fibers. >> patterns of the three materials are compared in Figure 2. The spectrum of Windform XT shows a broad hump in the range of 2θ from 15° to 30° and only an intense peak at 2θ of 21.5°; on the contrary, the XRD spectrum of Windform SP shows two peaks emerging from the hump at 2θ of 20° and 23.5°, respectively. In both cases the broad signal is characteristic of amorphous structures, showing that the material under investigation is not completely crystalline. Moreover, it is well known from the literature[23, 24] that polyamides can crystallize in the two so-called α and γ forms. The former shows a monoclinic or triclinic lattice, whereas the γ-form consists of a pseudohexagonal packing. X-ray diffraction spectrum of Windform XT 2.0 shows the presence of γ form only, while the two peaks observed in Windform SP can be attributed to α crystalline structure.

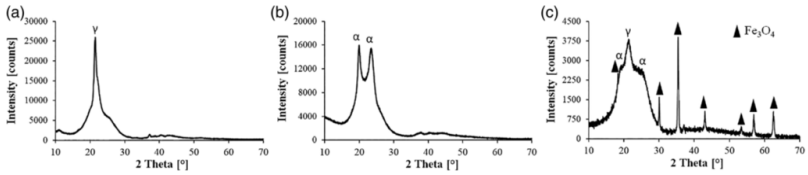

Figure 2 XRD patterns of (a) Windform XT, (b) Windform SP, and (c) Carbon PA

The XRD spectrum of Carbon PA is more complex than those observed for Windform materials since both the two crystalline phases of polyamide (α and γ forms) are present; in addition, several sharp peaks that can be attribute to magnetite can be observed. It is reported in the literature that this oxide can be added as a filler to polymeric-based matrices for specific applications: in automotive field it is used to make high-density components for sound damping. In addition, its high specific heat capacity, and then its capability to absorb and release large amount of heat, is exploited for green building applications.[25]

Thermal gravimetric analyses were performed under argon atmosphere with the aim of causing the pyrolysis of the matrix and then evaluating the content of reinforcing carbon fillers left as a residue.

The TGA curves for the three composite materials under investigation are compared in Figure 3. It shows that all the polyamide matrices start their thermal degradation at similar temperatures: 360°C for Windform XT, 355°C for both Windform SP and Carbon PA. After the matrix thermal decomposition, a residue is left: in the case of Windform XT and Windform SP, it is mainly composed by the reinforcing carbon fibers and a small additional amount of carbonaceous materials resulting from the polymeric matrix pyrolysis. The repetition of the TGA test in air for these two materials shows that the residue left from the combustion of polymer matrix and carbon fibers is negligible, thus proving that these materials do not contain inorganic fillers. A TGA test performed on unfilled polyamide up to 1,000°C in argon atmosphere left a residue lower than 1wt%, thus suggesting that the residue left after the test in inert atmosphere is representative of the fiber concentration. According to this procedure, a fiber concentration of about 28 and 19 wt% was found for Windform XT and Windform SP, respectively.

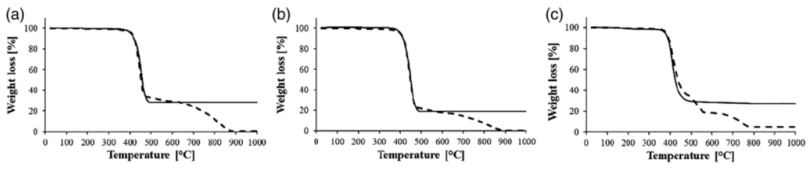

Figure 3 TGA curves of (a) Windform XT, (b) Windform SP, (c) Carbon PA. The continuous curves are referred to TGA in argon atmosphere; the dashed curve was performed in flowing air

After the TGA analysis of Carbon PA under inert atmosphere a residue of 27.1 wt% was found that can be attributed to the fillers, namely carbon fibers and iron oxide. The amount of inorganic filler can be quantified by repeating the TGA test in air (Figure 3c, dashed curve). In this case both polymer and carbon fibers burn, so that the residue of 4.4 wt% can be attributed to the iron oxide. In this manner a carbon fiber concentration of 22.7 wt% was assessed.

The DSC curves obtained by heating the samples up to 250°C in argon atmosphere and then cooling down them to ambient temperature are depicted in Figure 4.

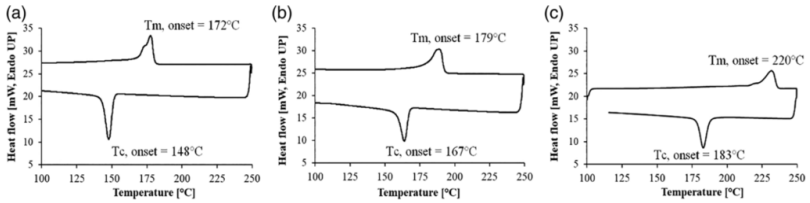

Figure 4 DSC curves of (a) Windform XT, (b) Windform SP, (c) Carbon PA

The heating curves of the three materials show an endothermic peak, which is related to the melting of the crystalline fraction of the polyamide matrix. This peak shows its onset at about 172°C for polyamide-12 (matrix of Windform XT), at 179°C for polyamide-11 (Windform SP matrix), and at 220°C for polyamide-6 (Carbon PA matrix), which is consistent with the literature data.[26] The cooling curves display an exothermal peak due to the crystallization from the melt. The onset of this peak is placed at 151°C, 167°C, and 183°C for polyamide-12, polyamide-11, and polyamide-6, respectively.

The range of temperature between the crystallization (during cooling) and the melting (during heating) is currently taken as a temperature window suitable for processing the material by SLS. These outcomes show as the processing of polyamide-11 should be performed in a narrower range of temperature with respect to polyamide-12.

Moreover, the DSC results allow to evaluate the crystalline fraction of the polymer matrix according to Equation (1):

$$\chi_c = \frac{\Delta H_m}{\Delta H_f^0 * (1 - f)} * 100, \quad (1)$$

where χ_c = fraction of crystalline material in the matrix of the composite; ΔH^0 = theoretical melting enthalpy for the mass unit of crystalline polyamide; ΔH_m = experimental enthalpy obtained from the melting peak and referred to mass unit of composite; $(1 - f)$ = fraction of the sample constituted by polyamide (f = weight fraction of fillers in the composite, previously evaluated by TGA).

Theoretical melting enthalpies of 209.2 J/g for polyamide-12 and of 189 J/g for both polyamide-11 and polyamide-6 were used for the calculation.[27–29] Weight percent of crystalline phase of 15, 25, and 18% were then estimated for polyamide-12, polyamide-11, and polyamide-6, respectively.

Composite samples were treated at 800°C in an inert atmosphere with the aim to cause the thermal decomposition of matrix and to recover the filler. The examination of the fillers by optical microscopy allowed

for detecting the length of the carbon fibers. The length of 200 fibers was measured for each sample, thus obtaining the statistical distribution of fiber length values. The results are summarized in Figure 5.

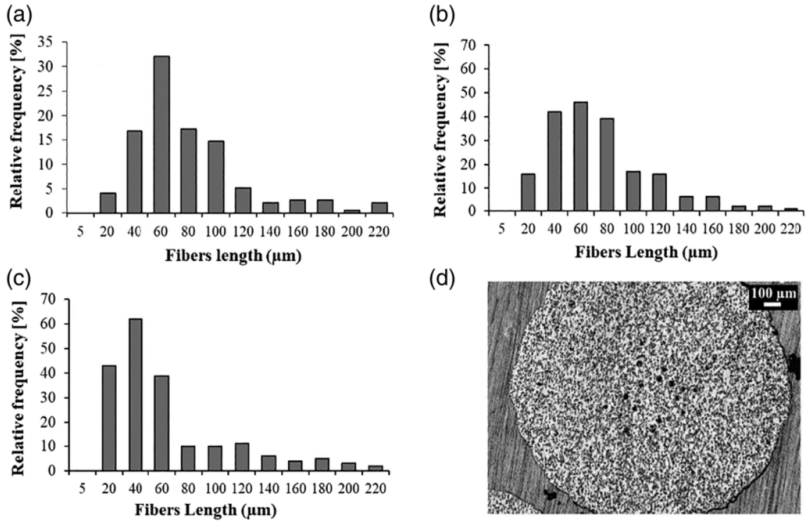

Figure 5 Fiber length distribution for: (a) Windform XT, (b) Windform SP, and (c) Carbon PA; Micrography of Carbon PA filament

In all samples, most of the fibers showed length lower than 180 µm, with an average value of 81.8, 75.5, and 77.0 µm for Windform XT, Windform SP, and Carbon PA, respectively. The fiber length distributions of Windoform XT and SP are quite similar showing an asymmetric trend; therefore, the fibers should give similar contribution to the materials strength when present in the same concentration. In addition, the measurement of fibers diameter reveals that the values observed for Windform SP and Winform XT are very similar (6.4 and 5.8 µm, respectively).

On the other hand, the fiber content was observed to be rather different in the two composites (as discussed above); as a consequence, these different concentrations should affect in a different manner the mechanical behavior of the materials.

Regarding the Carbon PA, the fibers length distribution (Figure 5c) shows an asymmetric curve where most of the fibers are in the range between 10 and 70 µm; the average diameter of the filaments is 1.6 mm and the embedded fibers show a diameter of about 5.3 µm.

Carbon PA filaments show an almost perfect alignment of the carbon fibers to the filament axis and some quite large porosities (size up to 30 µm) mainly placed in the central part of the filament (Figure 5d). The porosity inside the filaments very likely results in some porosity of the tensile specimens.

The orientation of the fibers is also expected to exert a significant influence on the mechanical behavior; for this reason, this feature was investigated as described in the next section.

3.2 Microstructure of tensile samples

3.2.1 Samples processed by SLS

The cross section of the tensile specimens processed according to different orientations is depicted in Figure 6 for Windform XT and Windform SP. Some porosities can be observed in particular inside samples built according to the ZX orientation. Only in this case, the layers are stacked perpendicularly to the tensile

sample axis and therefore the sample cross section is parallel to the layers. On the contrary, in the case of XY and YX orientations the layers are stacked parallel to the sample axis; as a consequence, the sample cross section cuts several layers and their interfaces. Considering that in XY and YX samples, the porosity level is lower than that observed for ZX orientation, it can be concluded that the layers are well bonded together and therefore there is not additional porosity at the layer interfaces.

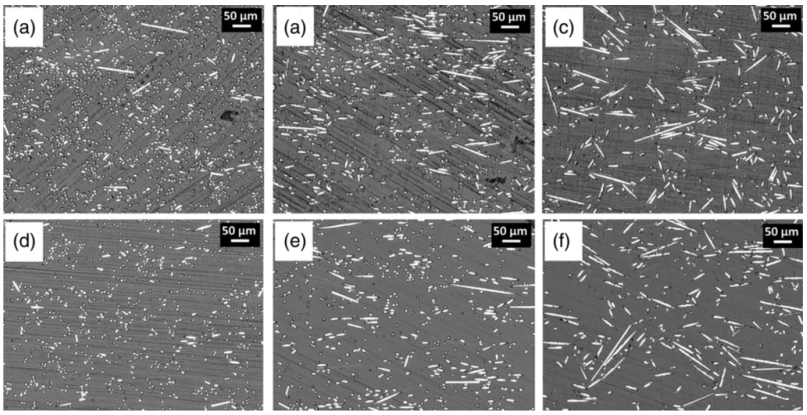

Figure 6 Cross section of the samples manufactured by SLS and built according to three orientations (XY-a and d, YX-b and e, and ZX-c and f). Samples of Windform XT on the upper line (a–b–c) and of Windform SP on the second one (d–e–f)

In Figure 6, the fibers are white, and the polymer matrix is gray. For both the composites, it is well evident that the fibers are differently placed with respect to the plane of section, depending on the adopted building orientation. In fact, the shape of the fiber sections depends on their orientation: the fibers, which are aligned to the sample axis, show a circular section, while the others show an elliptic shape. The length of these elliptical sections increases with the increase of the angle that the fibers form with the sample axis, reaching the maximum value when this angle is equal to 90°. Within the samples with XY orientation (Figure 6a,d) most of the fibers are parallel to the sample axis (and therefore show a circular section); on the contrary, in samples with ZX and YX orientation this preferential alignment of the fibers cannot be seen. In the last case (YX orientation), only few fibers are aligned to the sample axis; most of them form different angles with this axis and some of them are almost perpendicular to it. In addition, the fibers which show an elongated section (these fibers form a small angle with the section plane), tend to align parallel to the section plane direction. The fiber orientation is expected to affect both the stiffness and the strength of the tensile samples; the fibers, which are aligned to the sample axis, and therefore to the direction of the load application during the tensile test, should grant the best strengthening effect.

Reasonably, the different orientation of the fibers is caused by the movement of the recoater that always moves in the X direction; as a consequence, the fibers lying in every layer are aligned in this direction. Figure 7 depicts the expected effect of the recoater movement on fibers arrangement for specimens with different building orientations; in addition, the fiber placement in the sample cross sections was also reported.

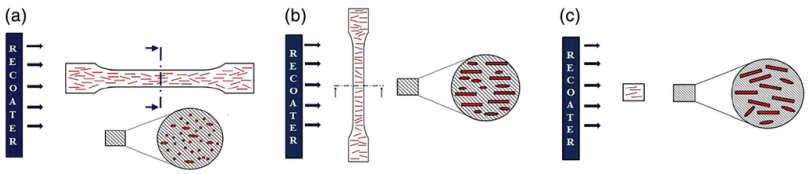

Figure 7 Effect of the recoater movement on the fiber orientation inside the tensile samples and on the sample cross section: (a) samples with XY built orientation, (b) samples with YX built orientation, (c) samples with ZX built orientation

3.2.2 Samples processed by FDM

The cross sections of the tensile specimens processed by FDM are shown in Figure 8.

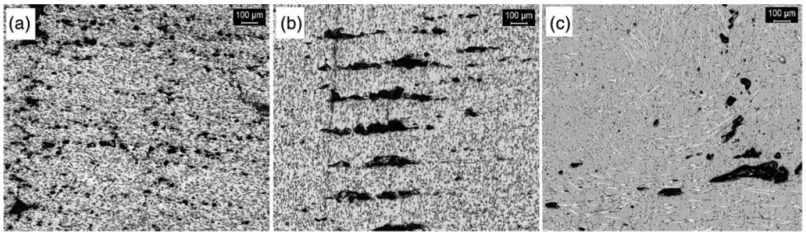

Figure 8 Cross sections of XY (a), XZ (b), and ZX (c) specimens

The cross section of the samples built along XY and XZ direction (Figure 8a,b) shows that the pores are aligned along some parallel directions. Very likely this feature means that porosity preferentially forms during the FDM process at the interfaces between the layers (see cross section of XY and XZ samples), and particularly near the sample contours where the filament bends when changing the deposition direction. This last feature is also evident in Figure 8c, which shows the cross section of ZX sample.

The arrangement of the carbon fibers can be observed on the cross section of tensile specimens by optical microscopy; the relevant scheme about the expected disposition of Carbon PA filaments inside these samples is shown in Figure 9.

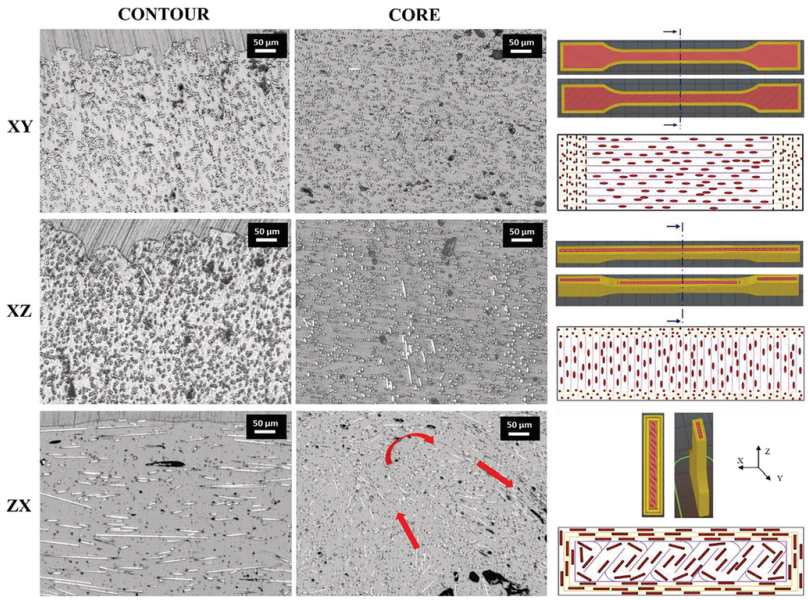

Figure 9 Orientation of fibers inside the tensile samples observed on the cross section of samples processed according to different orientations and schematic representation of expected specimen microstructures. Red arrows show as the fiber orientation changes as a function of the variation of the filament deposition direction

The building of specimens with orientations XY and XZ (definition of contours and subsequent filling of the layer core with a raster angle of 45°) should result in a specific orientation of both filaments and carbon fibers of respectively 0° at the contour and 45° at the sample core with respect to the sample axis.

The microstructure of XY an XZ samples cross section shows as the fibers placed at the contour are parallel to the axis of the specimen. Unfortunately, the different fiber orientation expected at the sample core cannot be well appreciated in the microstructure of sample cross section shown in Figure 9. In samples XY and XZ these fibers should form an angle of 45° with the sample axis and, therefore, their section should have an elliptical shape. Actually, it is easy to calculate that the 45° section of a fiber 5.5 μm in diameter should has the shape of an ellipse with major axis length of 7.8 μm, which is not very different from the fiber diameter. For this reason, the different shape of the fiber sections inside the two zones of the sample (contour and core) can be hardly appreciated.

In the case of the samples with ZX orientation, where the deposited layers are perpendicular to the sample axis, it is well evident that the fibers are parallel to the section plane and aligned at the contour; on the contrary, at the core they still lie on the section plane but are not placed parallel each other because the bending of the filaments during the layer building. Anyway, the samples manufactured according to the ZX orientation strongly differ from those showing XY and XZ orientations because there are not fibers parallel to the sample axis. On the contrary, in samples with XY and ZX orientation the fibers in the contour are parallel to the sample axis and the other fibers form with this axis an angle of about 45°.

The main difference from XY and XZ orientations deals with the relative proportion between the contour and the sample core: in fact, the contour constitutes large part of the specimen with XZ orientation, while in the case of XY orientation most of the sample is made by the core. Conclusively, a major fraction of fibers aligned to the axis of tensile sample should be present in XZ specimens with respect to the XY ones.

3.3 Mechanical features

3.3.1 Tensile test carried out at 0.1 mm/s strain rate

The results of tensile tests are summarized for the two materials processed by SLS (WindformXT and WindformSP) and that processed by FDM (Carbon PA) in Table 1. This table compares the results obtained for specimens built according to different orientations; the average values of elastic modulus, strength, and strain at failure and their standard deviations are here reported.

Table 1 Stiffness, strength, and deformation measured by tensile test carried out at 23°C and with strain rate of 0.1 mm/s

Sample orientation	Young modulus (MPa)	Tensile strength (MPa)	Strain at failure (%)
Windform® XT (SLS)			
XY	7,377 ± 155	82.56 ± 1.6	4.9 ± 0.6
YX	3,226 ± 149	58.55 ± 0.5	8.6 ± 0.6
ZX	3,232 ± 62	46.29 ± 3.0	5.7 ± 0.7
Windform® SP (SLS)			
XY	4,483 ± 221	65.6 ± 0.5	19.4 ± 0.7
YX	2,975 ± 128	55.0 ± 0.6	28.7 ± 2.6
ZX	2,335 ± 147	45.6 ± 0.6	11.8 ± 1.8
Carbon PA (FDM)			
XY	9,906 ± 617	97.7 ± 5.2	2.8 ± 0.9

Sample orientation	Young modulus (MPa)	Tensile strength (MPa)	Strain at failure (%)
XZ	9,360 ± 939	81.1 ± 5.2	1.7 ± 0.3
ZX	3,367 ± 305	39.3 ± 3.1	1.9 ± 0.3

The tensile test results in Table 1 put in evidence as the specimens processed by FDM (Carbon PA) show better stiffness and strength than specimens processed by SLS (Windform XT or Windform SP) when building orientations XY, YX, and XZ are considered; on the contrary, these three materials show similar behavior when the building orientation ZX is adopted.

It seems very hard to explain the superior tensile features of Carbon PA on the basis of the composite matrix characteristics, the total fiber concentration, the fiber length and the porosity; in fact, the percent of both matrix crystallinity and fiber concentration of Carbon PA is in between those of the two Windform materials, while the Carbon PA samples processed by FDM show shorter fibers and enhanced porosity with respect to those manufactured by SLS. Generally speaking, the mechanical behavior of polyamide-6 (Carbon PA matrix) is better that of both polyamide-11 and 12 (Windform matrices), but this feature is not sufficient to justify the superior stiffness and strength observed for FDM samples over SLS specimens. For instance, when samples with the XY orientations are compared, the Carbon PA shows a stiffness improvement from 220 to 37%, and a strength improvement from 49 to 18% with respect to the corresponding specimens produced by SLS. In addition, the higher porosity observed in Carbon PA could counterbalance the higher strength of polyamide 6. However, the additional inorganic filler that was found in Carbon PA material could also justify a different mechanical behavior. The most important difference between these samples deals with the processing technique; definitively FDM process gives better mechanical properties than SLS one.

The better strength and modulus of Windform XT with respect to Windform SP can be mainly ascribed to the higher fiber content (28 and 19 wt%, respectively).

The strain at failure for the different materials changes in the opposite manner than stiffness and strength: higher values of stiffness and strength correspond to lower deformation at failure. For example, strain of about 2% only was observed for Carbon PA, while much higher ductility was found for Windform samples.

Very important differences in the mechanical behavior resulted from the different orientation of the samples on the building platform. In every case, the ZX building orientation (which involves the deposition by FDM of the filaments and the alignment of the fibers during SLS process perpendicularly with respect to the tensile load) showed the worse mechanical performance. In this case, in addition to a low value of strength and stiffness, the strain at failure also decreased because failure mechanism is very likely based on the debonding of layers in correspondence of at some weaker interfaces.

The comparison of the mechanical properties of SLS samples with different orientations also show that the alignment of both the fibers and the layer interfaces to the tensile load direction granted the best mechanical behavior; for this reason, the orientation XY (fibers and layers parallel to the sample axis) resulted in better strength and stiffness than the orientation YX (layers parallel, but fibers perpendicular to the sample axis).

The difference in mechanical behavior between XY and XZ samples processed by FDM is not significant, if the standard deviation of experimental results is considered. On the other hand, both these two orientations entail the alignment of the filaments forming the contour to the sample axis, while the fibers in the sample core should be placed at 45° with respect to the sample axis. The only difference between FDM samples with XY and XZ orientations consists in the proportion between the infill and the contour, where the fibers are well aligned to the direction of the applied load and then better display their reinforcement effect. However, also the fibers placed at 45° inside the sample core probably can progressively align in the direction of the applied force during the tensile test progress, which reduces the microstructure and strength differences between samples with XY and XZ orientations.

Definitively, the FDM process seems to be able to ensure a more regular orientation of the carbon fibers than the SLS process. On one hand, the preferential orientation of the fibers maximizes the stiffness and the strength in the direction of the fibers; however, on the other hand, it enhances the anisotropic mechanical behavior of the material. A tailored architecture, obtained by varying the filament deposition direction for subsequent layers, could reduce this anisotropy.

In addition, the morphology of the fracture surfaces is affected by the orientation of the fibers with respect to the tensile sample axis, as shown in Figures 10 and 11.

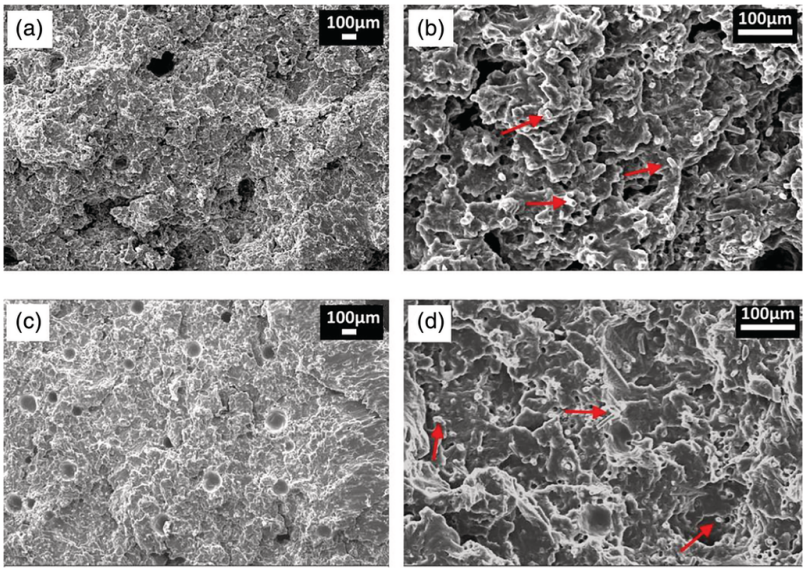

Figure 10 Fracture surface of SLS samples: Windform XT with XY orientation at ×50 (a) and ×200 (b); Windform SP with XY orientation at ×50 (c) and ×200 (d)

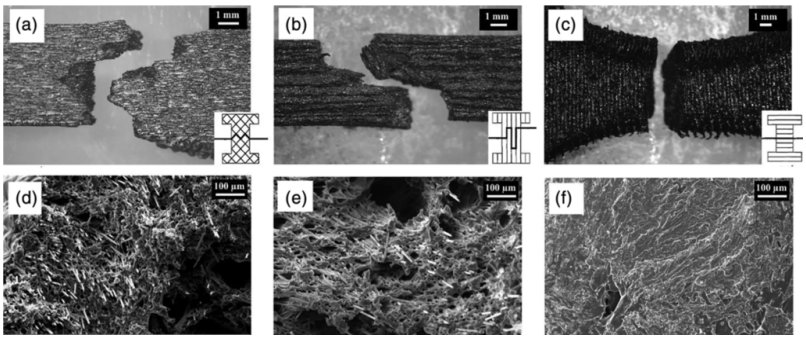

Figure 11 Fracture surfaces of: (a and d) Carbon PA with XZ orientation, (b and e) Carbon PA with XY orientation, (c and f) Carbon PA with ZX orientation, and expected crack propagation mechanism. Upper line: optical micrography and second line: SEM images

Porosity can be observed in both Windform samples when the fracture surface is observed at low magnification (Figure 10a,c). Pull-out of the fibers can be seen on the fracture surface when these fibers are placed parallel to the sample axis; this feature can be clearly detected for the materials processed by SLS (pulled out fibers are put in evidence by red arrows in Figure 10b,d) as well as for those manufactured by FDM (see Figure 11d,e). On the contrary, the fracture surface of samples showing both layers and fibers perpendicular to the sample axis are flat and without fibers (Figure 10f); very likely the decohesion at the

interface between adjacent layers is responsible for fracture and this mechanism results in flat fracture surfaces.

The fibers placed at 45° clearly affect the direction of crack propagation, this effect was observed for samples processed by FDM (Figure 10a,b).

3.3.2 Tensile test carried out at high strain rate

The outcomes of tensile tests performed at 23°C using a strain rate of 10 mm/s are summarized in Table 2. These tests performed at higher strain rate respect to the previous reported ones, confirm the hierarchy in terms of strength and modulus already observed for static tensile test: Carbon PA performs better than Windform XT, which in turn performs better than Windform SP. These tests also confirm the influence of the sample building orientation on the mechanical behavior of printed parts: a positive effect comes from the presence of carbon fibers placed parallel to the sample axis, while a detrimental effect is due to layer interfaces placed perpendicularly with respect to the sample axis.

Table 2 Tensile test performed at 23°C and with strain rate of 10 mm/s

Sample orientation	Young modulus (MPa)	Tensile strength (MPa)	Strain at failure (%)
Windform® XT, strain rate 10 mm/s			
XY	7,406 ± 136	90.9 ± 3.9	4.1 ± 0.3
YX	4,282 ± 132	67.8 ± 1.5	7.3 ± 0.7
ZX	3,236 ± 166	53.8 ± 1.0	4.7 ± 0.2
Windform® SP, strain rate 10 mm/s			
XY	4,818 ± 324	72.6 ± 1.0	16.5 ± 2.0
YX	3,002 ± 197	59.6 ± 1.5	27.6 ± 0.8
ZX	2,715 ± 61	54.3 ± 0.6	9.9 ± 1.7
Carbon PA, strain rate 10 mm/s			
XY	13,336 ± 1,428	139.0 ± 6.2	1.6 ± 0.2
XZ	12,161 ± 882	116.0 ± 5.1	1.3 ± 0.1
ZX	3,797 ± 151	42.8 ± 5.1	1.3 ± 0.2

Both the elastic modulus and the tensile strength were found to increase appreciably with the increase of the strain rate adopted during the tensile tests. This effect was observed for all the materials and for all the orientations investigated, whatever the processing method adopted (SLS or FDM). On the contrary, the strain at failure slightly decreased for all the materials and all their building orientations with the strain rate increase.

4 CONCLUSIONS

FDM and SLS were used to print polyamide-based composites with chopped carbon fibers and these techniques were found respectively to cause fiber alignment in the direction of filament deposition or of recoater movement.

For this reason, the fibers can be oriented differently inside the printed parts depending on the positioning of the component on the building platform. In our experiments, this feature resulted in nonisotropic mechanical behavior, as superior strength and stiffness were observed in the direction of fiber alignment. In contrast, these properties were about 60% lower when measured in the direction perpendicular to the fibers. The orientation of carbon fibers, occurring to a greater degree in the FDM process, exerted a major influence on the mechanical behavior, exceeding the effects produced by the matrix characteristics (kind of polyamide matrix, matrix crystallinity, and porosity degree) or by the fiber length and percentage. Furthermore, the placement of the layer interfaces (which depends on part orientation) affected the mechanical behavior because the fracture mechanism involved debonding between the stacked layers when the interfaces were placed perpendicular to the loading direction. In all the composites, investigated ductility was found to decrease with increasing stiffness and strength. For these reasons, the orientation of a composite component with respect to the building platform, and therefore the fiber positioning inside it, should be carefully considered when designing an additive manufacturing process, in order to grant a favorable orientation of the fibers in the directions where better mechanical properties are required.

ACKNOWLEDGMENT

This research did not receive any specific grant from funding agencies in the public, commercial, or not-for-profit sectors.

REFERENCES AND NOTES

[1] J.-P. Kruth, M.-C. Leu, T. Nakagawa, *CIRP Ann.* 1998, **47**, 525.

[2] D.-A. Türk, R. Kussmaul, M. Zogg, C. Klahn, B. Leutenecker-Twelsiek, M. Meboldt, *Procedia CIRP* 2017, **66**, 306.

[3] S. L. N. Ford, *J. Int. Commer. Econ.* 2014, **6**, 1.

[4] U. M. Dilberoglu, B. Gharehpapagh, U. Yaman, M. Dolen, *Procedia Manuf.* 2017, **11**, 545.

[5] P. Parandoush, D. Lin, *Compos. Struct.* 2017, **182**, 36.

[6] F. Ning, W. Cong, J. Qiu, J. Wei, S. Wang, *Composites, Part B* 2015, **80**, 369.

[7] <<Query: Please provide the “city location of publisher” for reference 7. Ans: Stafa-Zurich. Switzerland>>A. Salem Bala, S. bin Wahab, *Advanced Engineering Forum*, Vol. **16**, Trans Tech Publications, 2016, p. 33.

[8] E. Yasa, K. Ersoy, *Aircraft Technology*, InTech, Rijeka 2018, p. 147.

[9] J. R. C. Dizon, A. H. Espera Jr.., Q. Chen, R. C. Advincula, *Addit. Manuf.* 2018, **20**, 44.

[10] B. Caulfield, P. E. McHugh, S. Lohfeld, *J. Mater. Process. Technol.* 2007, **182**, 477.

[11] <<Query: Please provide the "city location of publisher, name of the publisher" for reference 11. Ans: Publisher: University of Texas
City of Publisher: Austin

Additional details: ISSN 1053-2153
>>M. S. Hossain, J. Ramos, D. Espalin, M. Perez, R. Wicker, *International Solid Freeform Fabrication Symposium: An Additive Manufacturing Conference. Austin, TX*, Vol. **2013** 2013, p. 380.

[12] A. K. Sood, R. K. Ohdar, S. S. Mahapatra, *Mater. Des.* 2010, **31**, 287.

[13] K. Senthilkumaran, P. M. Pandey, P. V. M. Rao, *Mater. Des.* 2009, **30**, 2946.

[14] <<Query: Please provide the "volume number" for reference 14. Ans: Vol. 1126, No. 1,>>J. D. Arguëllo-Bastos, O. A. González-Estrada, C. A. Ruiz-Florián, A. D. Pertuz-Comas, E. D. V-Ninõ, *J. Phys. Conf. Ser.* 2018, 1126.

[15] C. Kousiatza, D. Tzetzis, D. Karalekas, *Compos. Sci. Technol.* 2019, **174**, 134.

[16] J. M. Chacón, M. A. Caminero, P. J. Núñez, E. García-Plaza, I. García-Moreno, J. M. Reverte, *Compos. Sci. Technol.* 2019, **181**, 107688.

[17] G. Liao, Z. Li, Y. Cheng, D. Xu, D. Zhu, S. Jiang, J. Guo, X. Chen, G. Xu, Y. Zhu, *Mater. Des.* 2018, **139**, 283.

[18] <<Query: Please provide the "page range" for reference 18. Ans: 656-670>>Q. Li, W. Zhao, Y. Li, W. Yang, G. Wang, *Polymers (Basel)* 2019, **11**.

[19] R. B. Floersheim, G. Hou, K. Firestone, *Rapid Prototyp. J.* 2009, **15**, 339.

[20] B. P. Heller, D. E. Smith, D. A. Jack, *Addit. Manuf.* 2016, **12**, 252.

[21] H. L. Tekinalp, V. Kunc, G. M. Velez-Garcia, C. E. Duty, L. J. Love, A. K. Naskar, C. A. Blue, S. Ozcan, *Compos. Sci. Technol.* 2014, **105**, 144.

[22] T. Mulholland, S. Goris, J. Boxleitner, T. Osswald, N. Rudolph, *J. Compos. Sci.* 2018, **2**, 45.

[23] K. Inoue, S. Hoshino, *J. Polym. Phys.* 1973, **11**, 1077.

[24] L. Li, M. H. J. Koch, W. H. De Jeu, *Macromolecules* 2003, **36**, 1626.

[25] C. De Armitt, *Polymers and Polymeric Composites: A Reference Series*, Springer, Berlin, Heidelberg 2016, p. 1.

[26] <<Query: Please provide the “city location of publisher” for reference 26. Ans: Pisa, Italia >>A. Ciaperoni, A. Mula, *Chimica e tecnologia delle poliammidi*, Pacini, 2001.

[27] S. Gogolewski, K. Czerntawska, M. Gastorek, *Colloid Polym. Sci.* 1980, **258**, 1130.

[28] P. Frübing, A. Kremmer, R. Gerhard-Multhaupt, A. Spanoudaki, P. Pissis, *J. Chem. Phys.* 2006, **125**, 214701.

[29] C. Millot, L.-A. Fillot, O. Lame, P. Sotta, R. Seguela, *J. Therm. Anal. Calorim.* 2015, **122**, 307.